https://doi.org/10.5194/egusphere-2026-2021
Preprint. Discussion started: 14 April 2026


# Chlorophyll-a concentration effects on equatorial Atlantic Ocean mean-state and interannual variability

Arthur Prigent[1,2], Riccardo Farneti[1], Manfredi Manizza[3], and Rodrigue Anicet Imbol Koungue[4]

[1]The Abdus Salam International Centre for Theoretical Physics, Trieste, Italy
[2]Now at: University of Brest, CNRS, Ifremer, IRD, Laboratoire d'Océanographie Physique et Spatiale (LOPS), IUEM, Plouzané, France
[3]National Institute of Oceanography and Applied Geophysics - OGS, Trieste, Italy
[4]Geophysical Institute, University of Bergen and Bjerknes Centre for Climate Research, Bergen, Norway

**Correspondence:** Arthur Prigent (arthur.prigent@univ-brest.fr)

**Abstract.** Chlorophyll-a concentration is known to influence the mean-state and interannual sea surface temperature (SST) variability of the tropics. Here, we investigate this effect in the equatorial Atlantic Ocean using a suite of ocean model simulations. In these simulations, the prescribed monthly climatology of chlorophyll-a concentration is multiplied by a factor ranging from 0.01 to 2. We find that a 'clear-ocean' simulation, i.e an ocean simulation with the monthly climatology of chlorophyll-a concentration multiplied by 0.01, results in a significantly warmer (+ 0.15 °C) eastern equatorial Atlantic SST and in a reduced (14%) amplitude of SST seasonal cycle when compared against a simulation with realistic chlorophyll-a levels. Additionally, the equatorial Atlantic vertical temperature gradient is weakened, the mixed-layer and thermocline are deepened, and equatorial upwelling is reduced. These changes in the mean-state of the 'clear-ocean' simulation lead to a significant reduction (12.9%) in eastern equatorial Atlantic SST variability. We also show that when the prescribed monthly climatology of chlorophyll-a concentration is scaled by 0.01, 0.5, 1, 1.5, and 2, the eastern equatorial Atlantic SST variability responds non-linearly. Our results also suggest that the ongoing observed decrease in tropical Atlantic chlorophyll-a concentration may weaken the interannual variability of SST.

## 1 Introduction

The tropical Atlantic Ocean exhibits a marked interannual sea surface temperature (SST) variability driven by the Atlantic zonal mode, also called Atlantic Niño (Zebiak, 1993; Lübbecke et al., 2018; Richter and Tokinaga, 2021). Atlantic Niños (Niñas) are extreme warm (cold) events characterized by large deviations from the seasonal cycle and typically occurring during May-June-July (MJJ) in the eastern equatorial Atlantic (ATL3 region; 20°W-0°E, 3°S-3°N). In addition, a secondary peak in interannual SST variability is observed in November-December (ND), referred to as Atlantic Niño II (Okumura and Xie, 2006). The underlying dynamics of the Atlantic Niño share similarities with the El Niño-Southern Oscillation (ENSO) in the Pacific Ocean (Servain et al., 1982; Keenlyside and Latif, 2007). Both climate modes involve a coupling of SST anomalies, zonal wind stress, and ocean heat content as described by the Bjerknes feedback loop (Bjerknes, 1969).

https://doi.org/10.5194/egusphere-2026-2021
Preprint. Discussion started: 14 April 2026


Atlantic Niños/Niñas can affect the climate of the neighboring continents (Hirst and Hastenrath, 1983), for example by modifying the onset of the West African Monsoon (Caniaux et al., 2011; Brandt et al., 2011) or influencing the Indian Monsoon (Kucharski et al., 2008). These events can also impact local marine ecosystems (Grodsky et al., 2008; Chenillat et al., 2021) as well as the sea-air $CO_2$ flux (Koseki et al., 2023). Therefore, enhancing our understanding of the Atlantic Niño mode, and its future evolution, is of particular socio-economic importance.

Atlantic Niños/Niñas occur in the equatorial Atlantic upwelling system (Brandt et al., 2023), which is rich in phytoplankton. Phytoplankton are aquatic photosynthetic organisms that form a crucial component of the global biogeochemical system and the basis of the marine food chain. Their presence in the water column affects the absorption of shortwave radiation, thereby influencing the vertical distribution of shortwave heating in the upper ocean (Lewis et al., 1990). Changing water clarity in coupled model simulations has been shown to result in significant changes in the global climate and circulation (Gnanadesikan and Anderson, 2009). Chlorophyll-a concentration (Chl-a hereafter) is typically used as a proxy for phytoplankton because it is the primary pigment involved in the photosynthesis of phytoplankton. In addition, Chl-a is well observed by satellites (Yoder and Kennelly, 2003), and it has been used to parameterize the effect of phytoplankton on solar radiation absorption in ocean and coupled models (Lewis et al., 1990; Morel and Antoine, 1994; Manizza et al., 2005). The impact of this effect on the mean-state and interannual variability of the tropical Pacific Ocean has been examined in observations (Strutton and Chavez, 2004) and extensively studied using ocean model experiments (Nakamoto et al., 2001; Murtugudde et al., 2002; Manizza et al., 2005; Sweeney et al., 2005; Park et al., 2014b, a) as well as coupled ocean-atmosphere-biogeochemistry models (Lengaigne et al., 2007; Anderson et al., 2009; Park et al., 2014b, a). However, despite the number of studies, their results remain somewhat contradictory (a summary can be found in Park et al. (2014b)). Some studies found an increased in eastern equatorial Pacific SST in the presence of Chl-a (Murtugudde et al., 2002; Marzeion et al., 2005) whereas others found a decrease (Manizza et al., 2005; Sweeney et al., 2005; Nakamoto et al., 2001; Löptien et al., 2009; Anderson et al., 2007, 2009; Jochum et al., 2010). Similarly, there is no consensus regarding the response of ENSO variability to the presence of Chl-a: it may either amplify ENSO (Marzeion et al., 2005; Lengaigne et al., 2007; Löptien et al., 2009; Anderson et al., 2009; Park et al., 2014b, a) or dampen it (Timmermann and Jin, 2002; Wetzel et al., 2006; Jochum et al., 2010).

The effects of this bio-physical process have received less attention in the tropical Atlantic Ocean, although the seasonal cycle of Chl-a in the eastern equatorial Atlantic is more pronounced than that of the eastern equatorial Pacific (Brandt et al., 2025). Frouin et al. (2007) compared an ocean general circulation model with constant Chl-a of 0.02 $\mathrm{mg\,m^{-3}}$ to a simulation with time and spatially varying Chl-a. They found in the simulation with varying Chl-a a cooling in the northern part of the Benguela upwelling system, an enhanced Equatorial undercurrent and strengthened Benguela current, as well as an increased meridional circulation in the upper 50 m and a decrease below 50 m. Similarly, Hernandez et al. (2017) compared a regional ocean model configuration with a constant and horizontally homogeneous Chl-a of 0.05 $\mathrm{mg\,m^{-3}}$, i.e. depleted water, to a simulation with a realistic monthly climatology of Chl-a. They found that relative to the low Chl-a simulation, the realistic simulation featured a cooling in the eastern equatorial Atlantic as well as in the Benguela and Senegalo-Mauritanian upwelling systems. Yet, to our knowledge the response of the interannual SST variability to the presence of Chl-a has not yet been examined in the equatorial Atlantic.

https://doi.org/10.5194/egusphere-2026-2021
Preprint. Discussion started: 14 April 2026


Here, we aim to investigate the equatorial Atlantic interannual SST variability response to this bio-physical process through ocean model experiments forced with different monthly Chl-a climatology. Specifically, this study addresses the following questions: 1) What are the effects of Chl-a on the mean-state of the equatorial Atlantic Ocean? 2) How would interannual SST variability in the equatorial Atlantic respond if Chl-a were nearly zero, halved or doubled?

To explore these questions, we present the different datasets, model configuration, and strategy used in Sect. 2. In the tropical Atlantic, the interannual SST variability is linked to the mean state. Therefore, we first examine the response of the tropical Atlantic mean-state to varying monthly climatology of Chl-a in Sect. 3.1. Then, we investigate the equatorial Atlantic interannual SST variability response to the presence of Chl-a in Sect. 3.2. Finally, we provide a summary and a discussion of the main results in Sect. 4.

## 2 Data and methods

### 2.1 Data

#### 2.1.1 Observational data

The monthly mean SST data from the Optimum Interpolation SST version 2.1 (Reynolds et al., 2007, OI-SST) produced by the Physical Sciences Laboratory of the National Oceanic and Atmospheric Administration (NOAA) available at 0.25° horizontal resolution from September 1981 to present day is used as a reference dataset. Monthly means of Chl-a are derived from the daily gap-free product Copernicus-GlobColour (Copernicus, 2024), available at 4 km horizontal resolution from 4th of September 1997 to present day. More information on the performance of this product and on the methods used to merge the different satellite measurements and to fill the gaps can be found in the "User manual" and "Quality information" at https://data.marine.copernicus.eu/product/OCEANCOLOUR_GLO_BGC_L4_MY_009_104/description.

#### 2.1.2 Ocean model configuration

To investigate the effect of Chl-a on the equatorial Atlantic mean-state and its interannual variability, we employed the NOAA-Geophysical Fluid Dynamics Laboratory Modular Ocean Model version 5 (Griffies, 2012, MOM5). MOM5 is a free-surface primitive-equation model and uses z* rescaled geopotential coordinate. The model configuration for the control run (ICTP-MOM5-CTRL) corresponds to: 1° horizontal resolution with 50 vertical levels, subgrid mesoscale processes are parametrized with the Gent-McWilliams skew-flux closure scheme (Gent and Mcwilliams, 1990; Gent et al., 1995; Griffies, 1998) and submesoscale eddy fluxes according to Fox-Kemper et al. (2008) and Fox-Kemper et al. (2011). Vertical mixing is represented with a K-profile parameterization (Large et al., 1994). The atmospheric forcing used is the JRA-55-based surface dataset for driving ocean-sea-ice models (Tsujino et al., 2018, JRA55-do) over the period from January 1958 to December 2021. Additionally, ICTP-MOM5-CTRL includes a monthly climatology of Chl-a, which is based on 8-day composites of Sea-viewing Wide Field-of-view Sensor (SeaWiFS) imagines taken from 1999 to 2001. The climatological mean field of this

https://doi.org/10.5194/egusphere-2026-2021
Preprint. Discussion started: 14 April 2026


dataset is shown in Fig. 1a. More details on the production of this climatology can be found in Griffies (2012). A validation of this model configuration for the equatorial Atlantic Ocean can be found in Prigent and Farneti (2024).

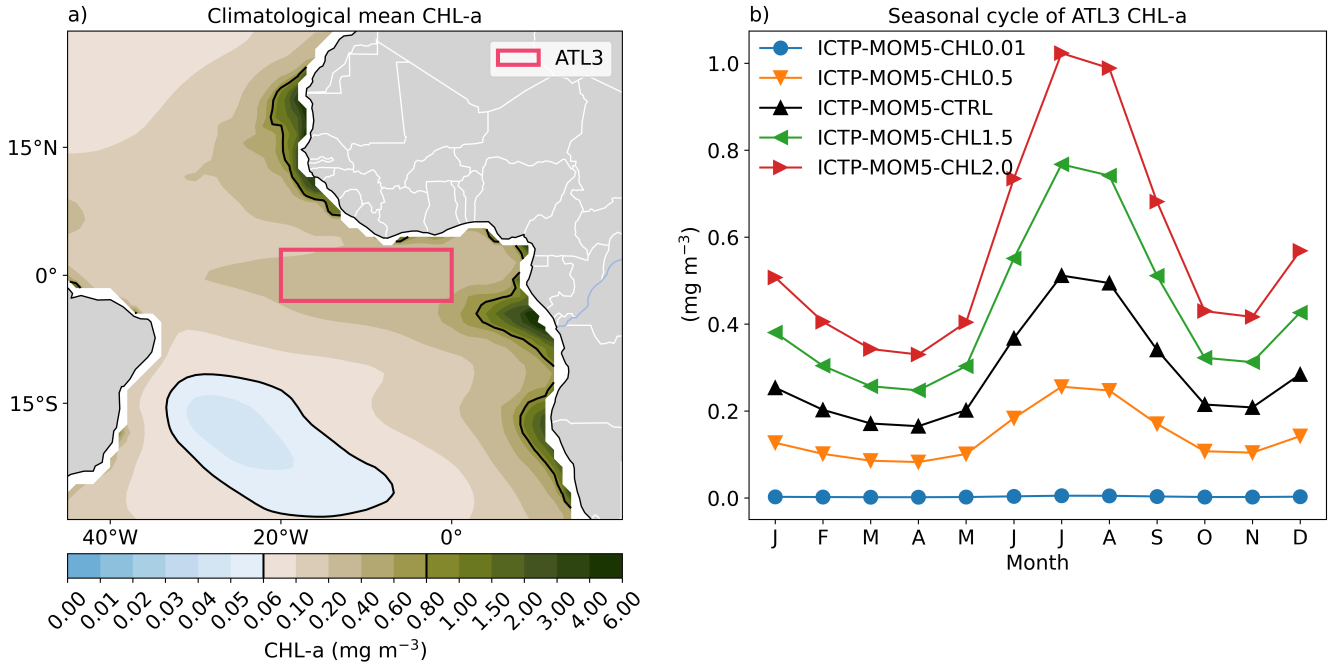


**Figure 1.** (a) Climatological mean chlorophyll-a concentration prescribed to ICTP-MOM5-CTRL. Black contours indicate the 0.06 mg m$^{-3}$ and 0.80 mg m$^{-3}$ chlorophyll-a concentration levels. (b) Seasonal cycle of the prescribed chlorophyll-a concentration averaged over the ATL3 (20°W-0°E, 3°S-3°N) region and for the different model simulations: ICTP-MOM5-CHL0.01 (blue), ICTP-MOM5-CHL0.5 (orange), ICTP-MOM5-CTRL (black), ICTP-MOM5-CHL1.5 (green), and ICTP-MOM5-CHL2.0 (red).

In ICTP-MOM5-CTRL, the effect of the presence of phytoplankton on the light absorption is based on Chl-a following Manizza et al. (2005). The total surface irradiance, $I_0$, is first split in two wavelength bands (as in Paulson and Simpson (1977)): the infrared ($I_{ir}$) and visible ($I_{vis}$), with a light partitioning of $I_{ir} = 0.58 \times I_0$ and $I_{vis} = 0.42 \times I_0$. Then, the visible part of the light is further split in two averaged wavelength bands (red ($I_{red}$) and blue/green ($I_{bg}$)), with $I_{red} = I_{bg} = I_{vis}/2$. This leads to a shortwave penetration at depth z ($I(z)$) of:

$$I(z) = I_{ir} \times e^{-k_{ir}z} + I_{red} \times e^{-k_{red}z} + I_{bg} \times e^{-k_{bg}z} \quad (1)$$

where $k_{ir}$, $k_{red}$, and $k_{bg}$ are light attenuation coefficients. Following Paulson and Simpson (1977), $k_{ir}$ = 2.86 m$^{-1}$, whereas $k_{red}$ and $k_{bg}$ depend on Chl-a as follows (Morel, 1988):

$$k_{red} = 0.225 + 0.037 \times [\text{Chl-a}]^{0.629} \quad (2)$$

$$k_{bg} = 0.0232 + 0.074 \times [\text{Chl-a}]^{0.674} \quad (3)$$

https://doi.org/10.5194/egusphere-2026-2021
Preprint. Discussion started: 14 April 2026


We note that, if a monthly climatology of surface Chl-a is provided to MOM5, this climatology is considered vertically uniform. This is certainly a limitation as the maximum Chl-a is usually found close to the nutricline.

## 2.2 Methods

### 2.2.1 Modelling strategy

To highlight the bio-physical effect on the equatorial Atlantic mean-state and interannual variability, we performed four sensitivity experiments identical to ICTP-MOM5-CTRL (see Sect. 2.1.2), except for the prescribed monthly climatology of Chl-a. In ICTP-MOM5-CHL0.01, the monthly climatology of Chl-a is multiplied by 0.01 and aims at simulating a 'clear-ocean', i.e. without Chl-a. In ICTP-MOM5-CHL0.5, the monthly climatology of Chl-a is reduced by 50%. In ICTP-MOM5-CHL1.5, it is increased by 50%, while in ICTP-MOM5-CHL2.0, the monthly climatology is doubled. For clarity, the prescribed monthly climatologies of Chl-a averaged over the ATL3 region are shown in Fig. 1b. In the following, we show the biological effect by analyzing the difference between ICTP-MOM5-CHL0.01 and ICTP-MOM5-CTRL. Differences between the other runs and ICTP-MOM5-CTRL are documented in the appendix.

### 2.2.2 Definition of anomalies, thermocline and mixed layer depths, and indexes

To obtain the detrended monthly mean anomalies, the raw data are first linearly detrended point-wise over the study period 1982/01-2020/12. Then, the monthly climatology of any variable is computed from the detrended data. Finally, the monthly climatology is subtracted to the detrended data to obtain the detrended monthly mean anomalies. Further, a 3-month centered running mean is applied to the detrended anomalies to attenuate the high-frequency variability. In order to preserve the length of the time series, the first and last values of the 3-month centered running mean are based on only two data points. The main regions of interest are the ATL3 region (20°W-0°; 3°S-3°N, red box on Fig. 2a) and the equatorial Atlantic (40°W-10°E; 3°S-3°N, blue box on Fig. 2a) where Atlantic Niños/Niñas occur. The maximum vertical temperature gradient ($\max(\partial T/\partial z)$) is used as a proxy for thermocline depth. The mixed-layer depth (MLD) is diagnosed through a density threshold criterion of 0.03 kg m$^{-3}$ increase from the reference value of surface potential density taken at 5 m depth (Griffies, 2012).

### 2.2.3 Significance test

To evaluate whether the variability (i.e. standard deviation of anomalies) or the mean state (time mean) of two simulations differ significantly, we use a bootstrap method. The null hypothesis ($H_0$) is that the difference between the two simulations is zero. The alternative hypothesis ($H_a$) is that the difference between the two simulations is non-zero. A bootstrap test is applied at each grid point. First, we compute the observed difference in mean state as the difference between the time means of the two models. Then, we generate a bootstrap distribution of possible mean-state differences by repeating the following process 5000 times: resampling the time indices with replacement independently for each model and recomputing the mean difference for each resampled dataset. We reject $H_0$ (and accept $H_a$) at the 99% confidence level if zero lies outside of the central 99%

https://doi.org/10.5194/egusphere-2026-2021
Preprint. Discussion started: 14 April 2026


interval of the bootstrap distribution (bounded by the 0.5th and 99.5th percentiles). To test differences in variability, we apply the same procedure but use the standard deviation instead of the mean, when creating the bootstrap distribution.

## 3 Results

### 3.1 Mean-state response

The response of the equatorial Atlantic Ocean mean-state to different monthly climatology of Chl-a is investigated by comparing ICTP-MOM5-CTRL against the different sensitivity experiments introduced in Sect. 2.1.2. Relative to ICTP-MOM5-CTRL, equatorial Atlantic SSTs in ICTP-MOM5-CHL0.01 are significantly warmer from 35°W to 2°E and between 2°S and 2°N (Fig. 2a). In the ATL3 region, the climatological mean SST difference between the two simulations amounts to 0.15 °C. We also note a surface warming along the Angolan and Namibian coasts as well as in the Senegalo-Mauritanian upwelling system (Fig. 2a), which is consistent with results from Hernandez et al. (2017). The ocean temperature differences between these two simulations are not restricted to the surface, as shown by the temperature section difference in the upper 250 m of the equatorial Atlantic (Fig. 2b). Compared to ICTP-MOM5-CTRL, ICTP-MOM5-CHL0.01 reveals a strong and statistically significant warming exceeding 2 °C within 50 m around the mean thermocline depth (Fig. 2b). This subsurface warming in the 'clear-ocean' simulation leads to a deepening of the maximum vertical temperature gradient and weakening of the vertical temperature gradient (Fig. 2c). A similar response is found when comparing ICTP-MOM5-CHL0.5 to ICTP-MOM5-CTRL, although with a smaller magnitude (Fig. A1d-f). Conversely, increasing the Chl-a by 50% and 100% leads to a slight, though not statistically significant, SST cooling (Fig. A1g,j). Furthermore, the equatorial Atlantic Ocean temperature and its vertical gradient in ICTP-MOM5-CHL1.5 and ICTP-MOM5-CHL2.0 only show moderate changes, characterized by subsurface cooling, enhanced vertical temperature gradient, and a slight shoaling of both the thermocline and MLD (Fig. A1g-l).

The eastern equatorial Atlantic SST is characterized by a pronounced seasonal cycle, with maximum values in February-March-April (FMA), when SSTs exceed 28 °C, and minimum values in July-August-September (JAS), when the Atlantic cold tongue develops and SSTs reach 25 °C or lower (Caniaux et al., 2011; Brandt et al., 2023). The amplitude of the seasonal cycle of SST is affected by the changes in vertical distribution of shortwave heating induced by the concentration of Chl-a (Fig. 2d). Compared to ICTP-MOM5-CTRL, the amplitude of the ATL3 SST seasonal cycle (defined as the difference between the FMA and JAS seasonal means) is reduced by 14% in ICTP-MOM5-CHL0.01, from 3.42 °C to 2.93 °C (Fig. 2d). This reduction mainly results from warmer SSTs in JAS (Fig. 2d), when the Chl-a usually peaks in the ATL3 region (Fig. 1b). ICTP-MOM5-CHL0.5 also simulates a reduction where the ATL3 SST seasonal cycle amplitude decreases by 4% relative to ICTP-MOM5-CTRL. On the contrary, ICTP-MOM5-CHL1.5 and ICTP-MOM5-CHL2.0 show only slight increases in the ATL3 SST seasonal cycle amplitude of 3% and 1%, respectively.

Comparing the ATL3 SST seasonal cycle from both control and sensitivity simulations to the one derived from OI-SST highlights the importance of taking into account the effect of the presence of phytoplankton onto the vertical distribution of shortwave heating. From Fig. 2d, the abundance of Chl-a contributes to reducing the warm bias, particularly in JAS, that is typical in ocean and climate models in this region (Richter et al., 2012; Farneti et al., 2022).

https://doi.org/10.5194/egusphere-2026-2021
Preprint. Discussion started: 14 April 2026


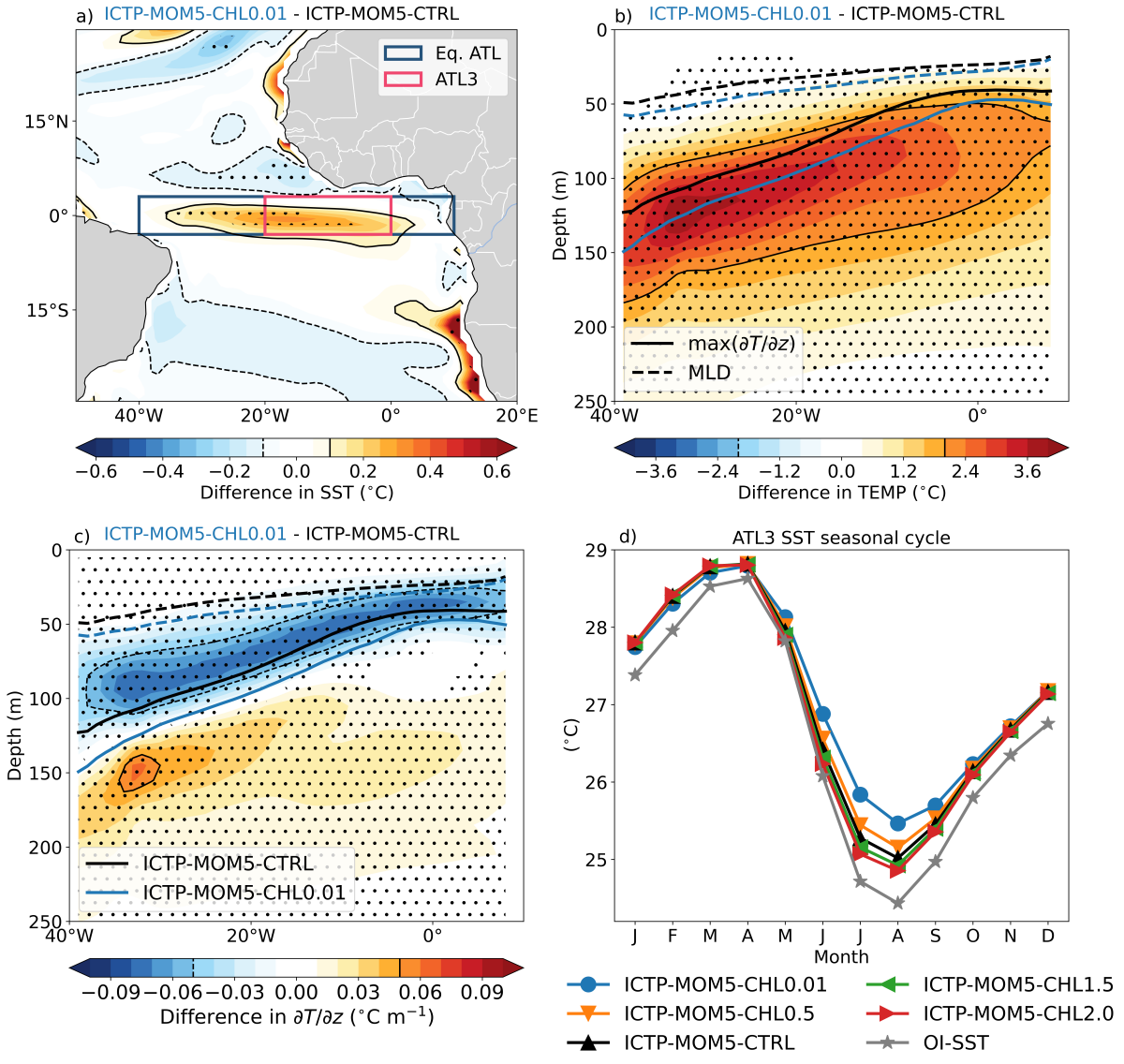


**Figure 2.** (a) Tropical Atlantic SST difference between ICTP-MOM5-CHL0.01 and ICTP-MOM5-CTRL. Black dashed (solid) contours indicate the -0.1 (0.1) °C difference. The blue and red boxes indicate the equatorial section (40°W-10°E; 3°S-3°N) used in (b, c) and the ATL3 region used in (d). (b) Upper 250 m equatorial Atlantic ocean temperature difference between ICTP-MOM5-CHL0.01 and ICTP-MOM5-CTRL. Black thick dashed and solid lines represent the MLD and max($\partial T/\partial z$) from ICTP-MOM5-CTRL, respectively. Similarly, the blue lines are for ICTP-MOM5-CHL0.01. Black dashed (solid) contours indicate the -2 (2) °C difference. (c) Same as (b) but for $\partial T/\partial z$. Black dashed (solid) contours indicate the -0.05 (0.05) °C m$^{-1}$ difference. Stippling in (a, b, c) indicate where the difference between the two simulations is significant at the 99% level according to a bootstrap test (See Sect. 2.2.3). (d) Seasonal cycle of SST averaged over the ATL3 region for each simulation and OI-SST.

https://doi.org/10.5194/egusphere-2026-2021
Preprint. Discussion started: 14 April 2026


The surface warming in the absence of Chl-a is somewhat counterintuitive (Fig. 2a), as a reduced absorption near the surface would be expected to lead to surface cooling locally. Such a counterintuitive response has already been observed for the equatorial Pacific Ocean in several studies (Manizza et al., 2005; Sweeney et al., 2005; Löptien et al., 2009; Park et al., 2014b, a). We note that in most previous studies, results were shown by comparing the model run with active bio-heating effect against a run without, which is opposite to what is done here. They showed that the dominant mechanism explaining the surface cooling is the vertical redistribution of shortwave heating by Chl-a, enhancing upper-ocean stratification, which then results in a shoaling of the mixed layer, and ultimately strengthens equatorial upwelling through poleward volume transports. Our findings are thus consistent, showing opposite results.

In ICTP-MOM5-CTRL, the meridional ocean velocity averaged over the MLD shows surface divergence close to the equator driven by trade winds (Fig. 3a), leading to equatorial upwelling (Fig. 3c). In ICTP-MOM5-CHL0.01, surface divergence is reduced (Fig. 3b), leading to weaker equatorial upwelling (Fig. 3d,e). As ICTP-MOM5-CHL0.01 and ICTP-MOM5-CTRL are forced with identical atmospheric forcing (See Sect. 2.1.2), the reduced surface divergence cannot be attributed to a wind-driven reduction in Ekman divergence. Instead, according to Equation 10 in Sweeney et al. (2005), a deeper mixed layer in the equatorial region can reduce the meridional mass transport within the mixed layer under the same wind forcing. Consistent with this mechanism, ICTP-MOM5-CHL0.01 features deeper MLDs than ICTP-MOM5-CTRL (grey contours in Fig. 3b; shadings in Fig. A2a, b). We note that changes in MLD in the other simulations are less important Fig. A2c-e. The deepening of the mixed layer is likely due to increased vertical mixing associated with Chl-a induced changes in the vertical distribution of shortwave heating. Ultimately, the reduced Ekman divergence results in a weaker equatorial upwelling (Fig. 3d,e), explaining the surface warming in the 'clear-ocean' simulation (Fig. 2a).

### 3.2 Interannual variability response

In addition to modifying the ocean mean-state, the presence of Chl-a can also affect interannual SST variability. Park et al. (2014a, b) showed that, in the equatorial Pacific Ocean, forced ocean model simulations without, or with reduced, Chl-a simulated weaker interannual SST variability than simulations with realistic Chl-a levels. In the following, we assess the effect of different levels of Chl-a on the equatorial Atlantic interannual SST variability (Fig. 4; Fig. A3).

ICTP-MOM5-CHL0.01 shows a statistically significant reduction in interannual SST variability in the central equatorial Atlantic, particularly between 30°W and 0°E (Fig. 4a). ICTP-MOM5-CHL0.5 (ICTP-MOM5-CHL1.5 and ICTP-MOM5-CHL2.0) also exhibits reduced (enhanced) interannual SST variability in the central equatorial Atlantic. However, these changes are not significant at the 99% level (Fig. A3).

The reduction in SST variability is also evident in the time series of the ATL3-averaged SSTA (Fig. 4c), with standard deviations of 0.31 °C for ICTP-MOM5-CTRL and of 0.27 °C for ICTP-MOM5-CHL0.01, corresponding to a 12.9% reduction. We note that interannual ATL3 SST variability in ICTP-MOM5-CTRL is underestimated compared to OI-SST, which has a standard deviation of the ATL3 SSTA of 0.38 °C over the period 1982-2020. This underestimation in the ocean model is likely due to the atmospheric forcing (JRA55-do), as shown by Prigent and Farneti (2024).

https://doi.org/10.5194/egusphere-2026-2021
Preprint. Discussion started: 14 April 2026


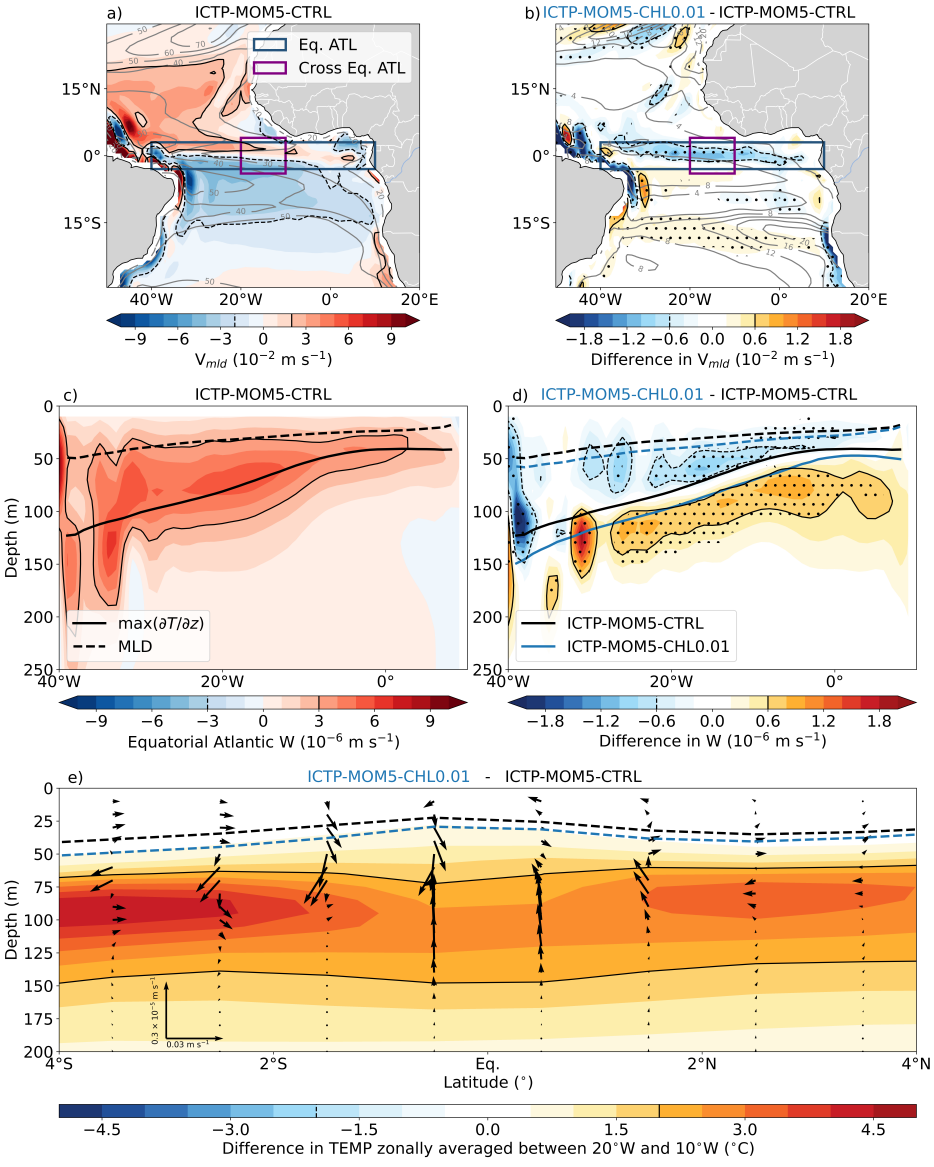


**Figure 3.** (a) Climatological mixed-layer meridional ocean velocity in ICTP-MOM5-CTRL. Black dashed (solid) contours show -2 (2) $\times 10^{-2}$ m s$^{-1}$. Grey contours show mean MLD (20 m to 80 m, 10 m interval). (b) Difference in mixed-layer meridional ocean velocity between ICTP-MOM5-CHL0.01 and ICTP-MOM5-CTRL, averaged over their respective MLDs. Black dashed (solid) contours show -0.6 (0.6) $\times 10^{-2}$ m s$^{-1}$. Grey contours show MLD differences (-20 m to 20 m, 4 m interval) (c) Climatological vertical velocity in the upper 250 m of the equatorial Atlantic (40°W-10°E; 3°S-3°N; blue box in (a)). Black solid contours denote 3 $\times 10^{-6}$ m s$^{-1}$. Black thick dashed and solid lines indicate the MLD and depth of max($\partial T/\partial z$), respectively. (d) Same as (c) but for the vertical velocity difference between ICTP-MOM5-CHL0.01 and ICTP-MOM5-CTRL. Black (blue) thick dashed and solid lines indicate the MLD and depth of max($\partial T/\partial z$) for ICTP-MOM5-CTRL (ICTP-MOM5-CHL0.01). (e) Cross-equatorial Atlantic section (4°S-4°N, zonally averaged between 20°W and 10°W; purple box in (a)) of temperature differences (shading) and meridional and vertical velocity differences (vectors; vertical velocity scaled by $10^4$).

https://doi.org/10.5194/egusphere-2026-2021
Preprint. Discussion started: 14 April 2026


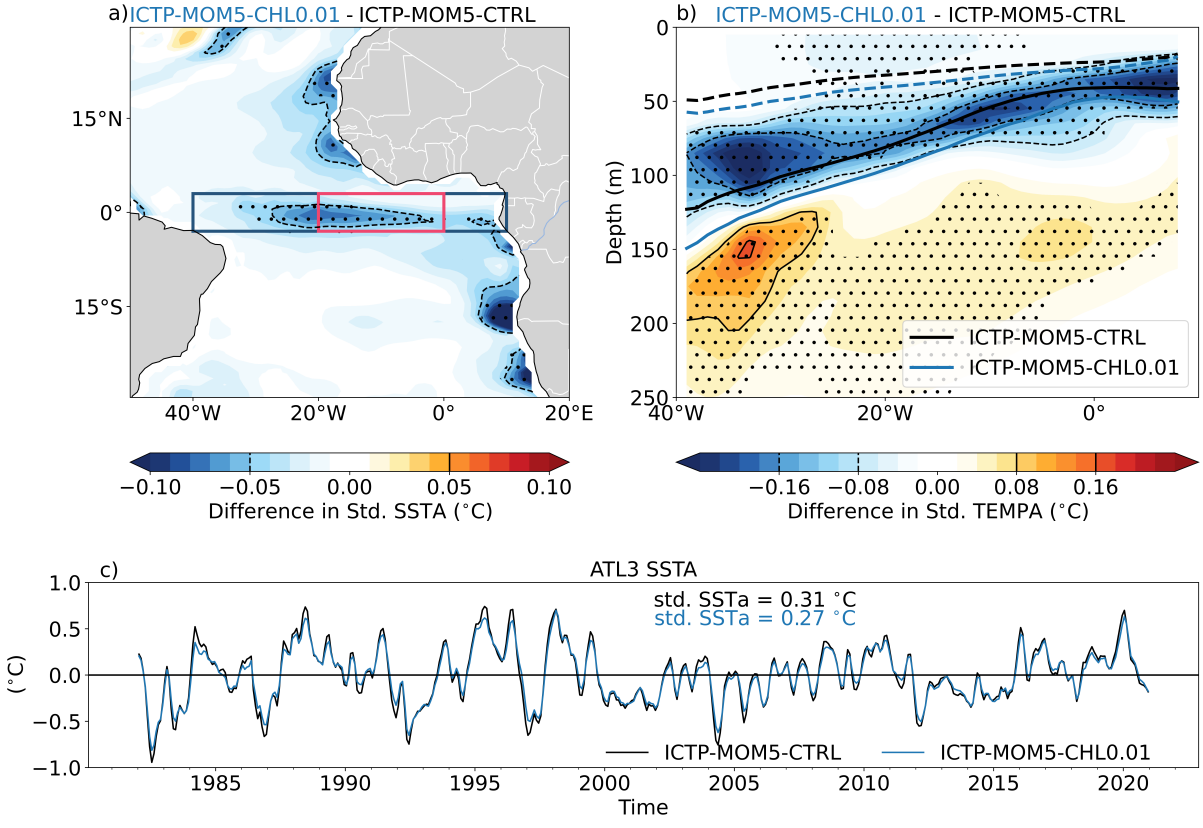


**Figure 4.** (a) Difference in the standard deviation of detrended SSTA between ICTP-MOM5-CHL0.01 and ICTP-MOM5-CTRL. Black dashed (solid) contours indicate -0.05 °C (0.05 °C). The blue and red boxes denote the equatorial Atlantic (Eq. ATL; 40°W–10°E, 3°S–3°N) and the ATL3 region (20°W–0°E, 3°S–3°N) regions, respectively. (b) Difference in the standard deviation of the upper 250 m of the equatorial Atlantic TEMPA between ICTP-MOM5-CHL0.01 and ICTP-MOM5-CTRL. Black dashed (solid) contours indicate -0.16 °C and -0.08 °C (0.08 °C and 0.16 °C). Black stipplings in (a) and (b) indicate regions where the difference in standard deviation is significant at the 99% level according to a bootstrap test (see Sect. 2.2.3). (c) Time series of detrended ATL3-averaged SSTA for ICTP-MOM5-CTRL (black) and ICTP-MOM5-CHL0.01 (blue).

https://doi.org/10.5194/egusphere-2026-2021
Preprint. Discussion started: 14 April 2026


The effect of Chl-a on interannual temperature variability is not restricted to the surface. The ocean temperature variability in the upper 150 m of the equatorial Atlantic (40°W-10°E; 3°S-3°N) is also significantly reduced in ICTP-MOM5-CHL0.01 (Fig. 4b). As all simulations are forced with identical winds, thermocline depth variations are similar across simulations (Fig. A4) and therefore cannot explain the changes in temperature variability. Instead, the reduced subsurface temperature variability in the vicinity of the thermocline is explained by a weakened and deepened vertical temperature gradient in ICTP-MOM5-CHL0.01 (Fig. 2c). Additionally, weakened equatorial upwelling (Fig. 3d) also contributes to the reduced interannual SST variability in ICTP-MOM5-CHL0.01. Similar but weaker reductions are found when comparing ICTP-MOM5-CHL0.5 to ICTP-MOM5-CTRL (Fig. A3c, d). In contrast, and although these changes are not statistically significant, both ICTP-MOM5-CHL1.5 and ICTP-MOM5-CHL2.0 exhibit increased subsurface temperature variability in the equatorial Atlantic (Fig. A3e-h), consistent with the enhanced vertical temperature gradient in those simulations (Fig. A1i,l).

Next, we examine the response of the interannual ATL3 SST variability as levels of Chl-a are varied. the response is strongest in MJJ and ND, which correspond to the peak seasons for the Atlantic Niño and Atlantic Niño II (Fig. 5a), respectively. The seasonal cycle of ATL3 SST variability is well captured by ICTP-MOM5-CTRL, although with too weak variability all year round (Fig. 5a). The response of the interannual ATL3 SST variability in MJJ to prescribed Chl-a is non-linear, with a quadratic fit explaining 98% of the variance (Fig. 5b). The ATL3 interannual SST variability in MJJ is of 0.345 °C in ICTP-MOM5-CTRL. Relative to this value, ICTP-MOM5-CHL1.5 and ICTP-MOM5-CHL2.0 show small increases of 2.29% and 3.76%, respectively, while ICTP-MOM5-CHL0.5 and ICTP-MOM5-CHL0.01 depict decreases of 3.27% and 13.47%, respectively.

The fact that changes in the mean state of Chl-a affect the interannual SST variability in the tropical Atlantic Ocean is of particular interest, as a merged satellite product of Chl-a shows marked trends over the period 1998-2024 (Fig. 5c). Similar trends have also been reported in recent studies (Zhao et al., 2025; Hong et al., 2025; Silsbe et al., 2025). Over that period, the eastern equatorial Atlantic Ocean exhibits decreasing trends in Chl-a (Fig. 5c). The timeseries of the Chl-a averaged over the ATL3 region reveals a clear reduction in the yearly maxima, while the yearly minima remain stable (Fig. 6a). Comparing the seasonal cycle of Chl-a averaged over the ATL3 region during 1998-2011 with the one obtained over 2012-2024 reveals that the largest decrease occur during July-August-September, the season of maximum Chl-a (Fig.6b). These ongoing changes in Chl-a in the tropical Atlantic Ocean underscore the need to improve our understanding of the relationship between Chl-a and interannual SST variability in the tropical Atlantic.

## 4 Discussion and Conclusions

We investigated the equatorial Atlantic mean-state and interannual variability responses to modified shortwave heating distributions induced by Chl-a using an ocean model and by carrying out a suite of sensitivity experiments. Our results showed significant responses when comparing a 'clear-ocean' simulation, including a satellite-based climatology of Chl-a multiplied by 0.01 (ICTP-MOM5-CHL0.01), to a 'realistic' simulation, using the same Chl-a climatology (ICTP-MOM5-CTRL).

Compared with ICTP-MOM5-CTRL, ICTP-MOM5-CHL0.01 simulates an equatorial Atlantic mean-state characterized by:

- A 0.15 °C warming and a 14% reduction of the amplitude of the SST seasonal cycle in the ATL3 region (Fig. 2).

https://doi.org/10.5194/egusphere-2026-2021
Preprint. Discussion started: 14 April 2026


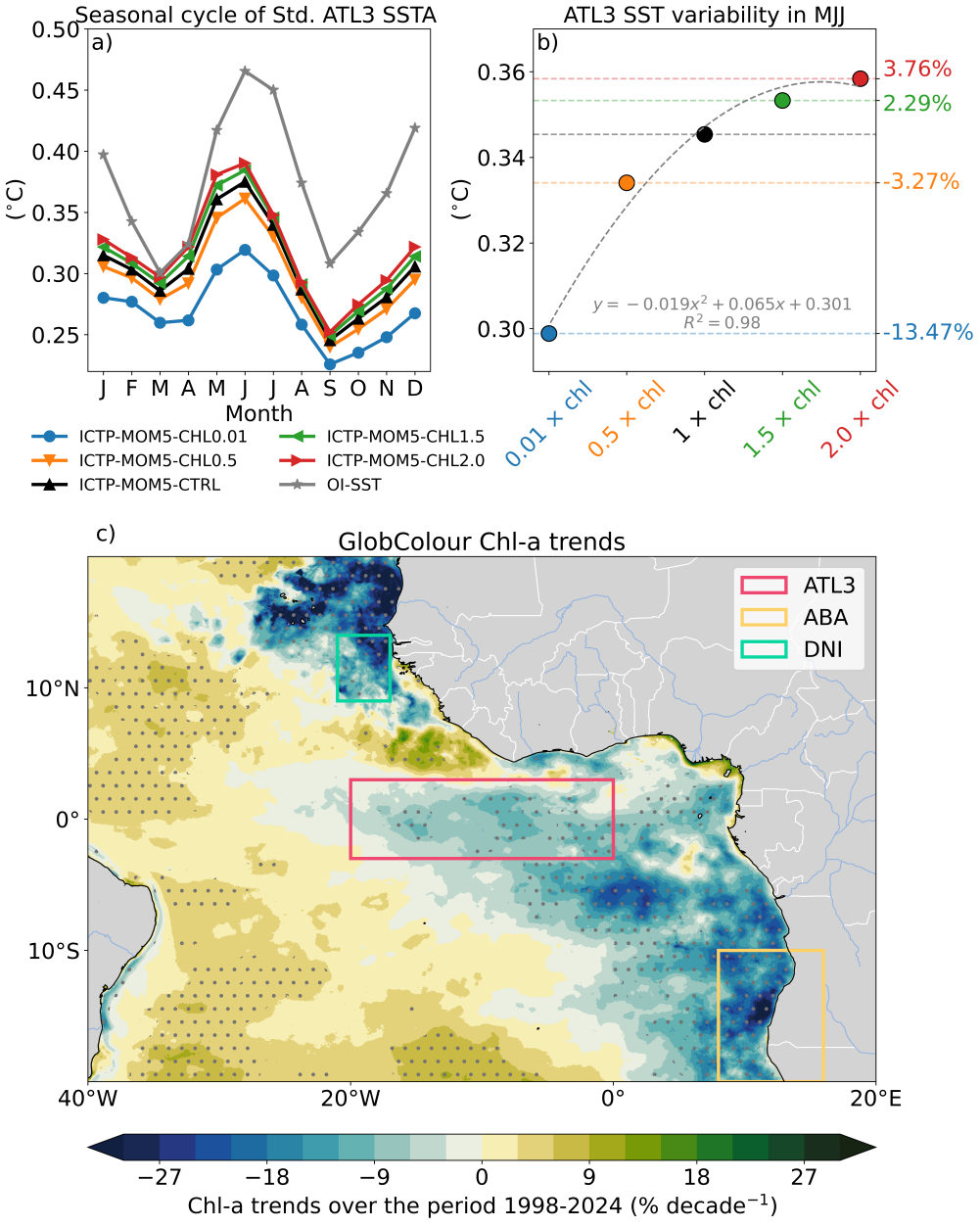


**Figure 5.** (a) Seasonal cycle of the standard deviation of the detrended SSTA averaged over the ATL3 region for ICTP-MOM5-CHL0.01 (blue), ICTP-MOM5-CHL0.5 (orange), ICTP-MOM5-CTRL (black), ICTP-MOM5-CHL1.5 (green) and ICTP-MOM5-CHL2.0 (red). The red, orange, and green boxes indicate the ATL3, ABA (8°E-16°E, 20°S-10°S), and DNI (21°W-17°W, 9°N-14°N) regions, respectively. (b) Scatter diagrams showing the standard deviation of SSTAs averaged over the ATL3 region in function of the prescribed Chl-a seasonal cycle as indicated on the x-axes. The right y-axis shows the percentage of change in SST variability relative to the ICTP-MOM5-CTRL value. (c) Linear trends in Chl-a over January 1998-December 2024. The trend is expressed in % decade$^{-1}$ and calculated from the linear slope evaluated using monthly means of the daily gap-free product, then multiplied by 120, divided by the climatological mean concentration at each grid point, and multiplied by 100. Grey stipplings indicate regions showing a statistically significant trend at the 95% level according to a Student's t-test.

https://doi.org/10.5194/egusphere-2026-2021
Preprint. Discussion started: 14 April 2026


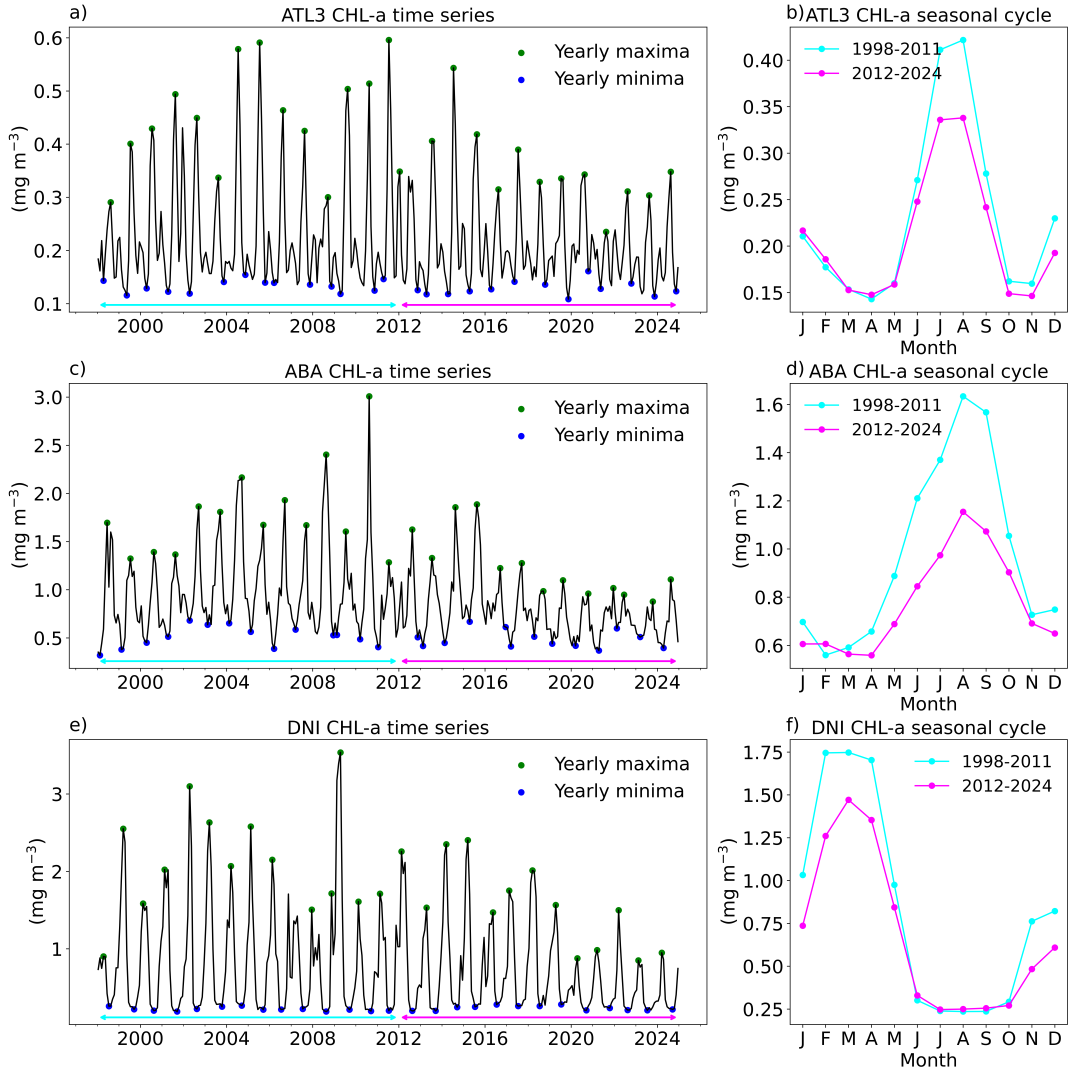


**Figure 6.** (a) Time series of chlorophyll-a concentration averaged over the ATL3 region from 1998/01 to 2024/12. Green (blue) dots indicate the yearly maxima (minima). The cyan (magenta) arrow denotes the period from 1998/01-2011/12 (2012/01-2024/12). (b) Seasonal cycle of the ATL3 chlorophyll-a evaluated over 1998-2011 (cyan) and 2012-2024 (magenta). (c, d) Same as (a, b) but for the ABA (orange box in Fig. 5c; 8°E-16°E, 20°S-10°S) region. (e, f) Same (a, b) but for the DNI (green box in Fig. 5c; 21°W-17°W, 9°N-14°N) region.

– A subsurface warming, along with a reduced vertical temperature gradient and deepened thermocline (Fig. 2).

– A deepened MLD in the equatorial region, leading to a reduction of the meridional mass transport and weakened equatorial upwelling, consistent with previous studies carried out in the equatorial Pacific (Sweeney et al., 2005; Löptien et al., 2009; Park et al., 2014b, a).

https://doi.org/10.5194/egusphere-2026-2021
Preprint. Discussion started: 14 April 2026


The response of interannual SST and subsurface temperature variability in the equatorial Atlantic to Chl-a–induced shortwave heating redistribution is assessed by comparing ICTP-MOM5-CHL0.01 with ICTP-MOM5-CTRL, revealing:

- A reduction of 12.9% of the ATL3 SST variability from 0.31 °C to 0.27 °C (Fig. 4a, c).
- A reduction of the equatorial Atlantic subsurface temperature variability (Fig. 4b), which is linked to changes in the vertical temperature gradient and equatorial upwelling.
- The reduction of the ATL3 SST variability is most pronounced in MJJ, with a reduction of 13.47% from 0.345 °C to 0.298 °C (Fig. 5a)

Furthermore, the analysis of additional simulations showed that the interannual SST variability in the equatorial Atlantic upwelling system responds non-linearly to different levels of Chl-a (Fig. 5b). By analyzing a merged satellite product of Chl-a we found that, over the period from 1998 to 2024, the Chl-a seems to be declining in the eastern equatorial Atlantic (Fig. 5c). We acknowledge that this decline in Chl-a has already been reported in recent studies (Zhao et al., 2025; Hong et al., 2025; Silsbe et al., 2025). Our results thus suggest that this decline could have contributed to the weakened interannual SST variability observed after 2000 in the ATL3 region (Prigent et al., 2020). We also note that the Chl-a is declining in the tropical Angolan and Senegalo-Mauritanian upwelling systems (Fig. 5c; Fig. 6). These two coastal regions exhibit large interannual SST variability driven by the extreme warm and cold coastal events, called Benguela Niños/Niñas for the tropical Angolan upwelling system (Shannon et al., 1986) and Dakar Niños/Niñas for the Senegalo-Mauritanian upwelling system (Oettli et al., 2016). Therefore, the link between interannual SST variability and Chl-a in those regions should be examined in further studies.

Since our model simulations were not coupled to a biogeochemical model, we could not investigate the potential impact of interannual variations in Chl-a concentration on interannual SST variability in the tropical Atlantic Ocean. Park et al. (2014a) showed that interannually varying Chl-a can have a damping effect on ENSO. In other words, during a La Niña event, trade winds are enhanced, leading to increased upwelling and supply of nutrients, which results in anomalously high Chl-a concentration that traps more solar radiation in the upper layer, thereby damping the negative SST anomaly. The opposite effect occurs during an El Niño event due to the reduction in nutrients supply. Such a damping effect is also likely active in the tropical Atlantic, as interannual variations in SST and Chl-a (or net primary production) have been found to occur concomitantly in the equatorial Atlantic (Grodsky et al., 2008; Chenillat et al., 2021), as well as in the tropical Angolan (Imbol Koungue et al., 2024) and Senegalo-Mauritanian (Imbol Koungue et al., 2025) upwelling systems. Therefore, further studies using coupled ocean-atmosphere-biogeochemical simulations are needed to investigate this damping effect in the tropical Atlantic Ocean.

*Code and data availability.* Codes to reproduce the figures are available upon request to the corresponding author. The OI-SST version 2.1 dataset can be accessed at https://psl.noaa.gov/data/gridded/data.noaa.oisst.v2.highres.html. The GlobColour dataset can be accessed at https://doi.org/10.48670/moi-00281. All ICTP-MOM5 simulations used in this study are archived on Zenodo and can be accessed at https://doi.org/10.5281/zenodo.18867384 (Farneti, 2026).

https://doi.org/10.5194/egusphere-2026-2021
Preprint. Discussion started: 14 April 2026


*Author contributions.* AP carried out the analyses and wrote the first draft of the paper. RF ran the sensitivity experiments. AP, RF, MM, RAIK participated in the conceptualization, editing, and reviewing of the paper.

*Competing interests.* The authors declare there are no conflicts of interest for this manuscript.

*Acknowledgements.* MM was supported by the National Recovery and Resilience Plan project TeRABIT (Terabit network for Research and Academic Big data in Italy - IR0000022 - PNRR Missione 4, Componente 2, Investimento 3.1 CUP I53C21000370006) in the frame of the European Union - NextGenerationEU funding. RAIK has received funding from the European Union's Horizon 2020 Research and Innovation Program for the project EcoCLimEx under the Marie Skłodowska-Curie grant agreement ID 101203635.

https://doi.org/10.5194/egusphere-2026-2021
Preprint. Discussion started: 14 April 2026


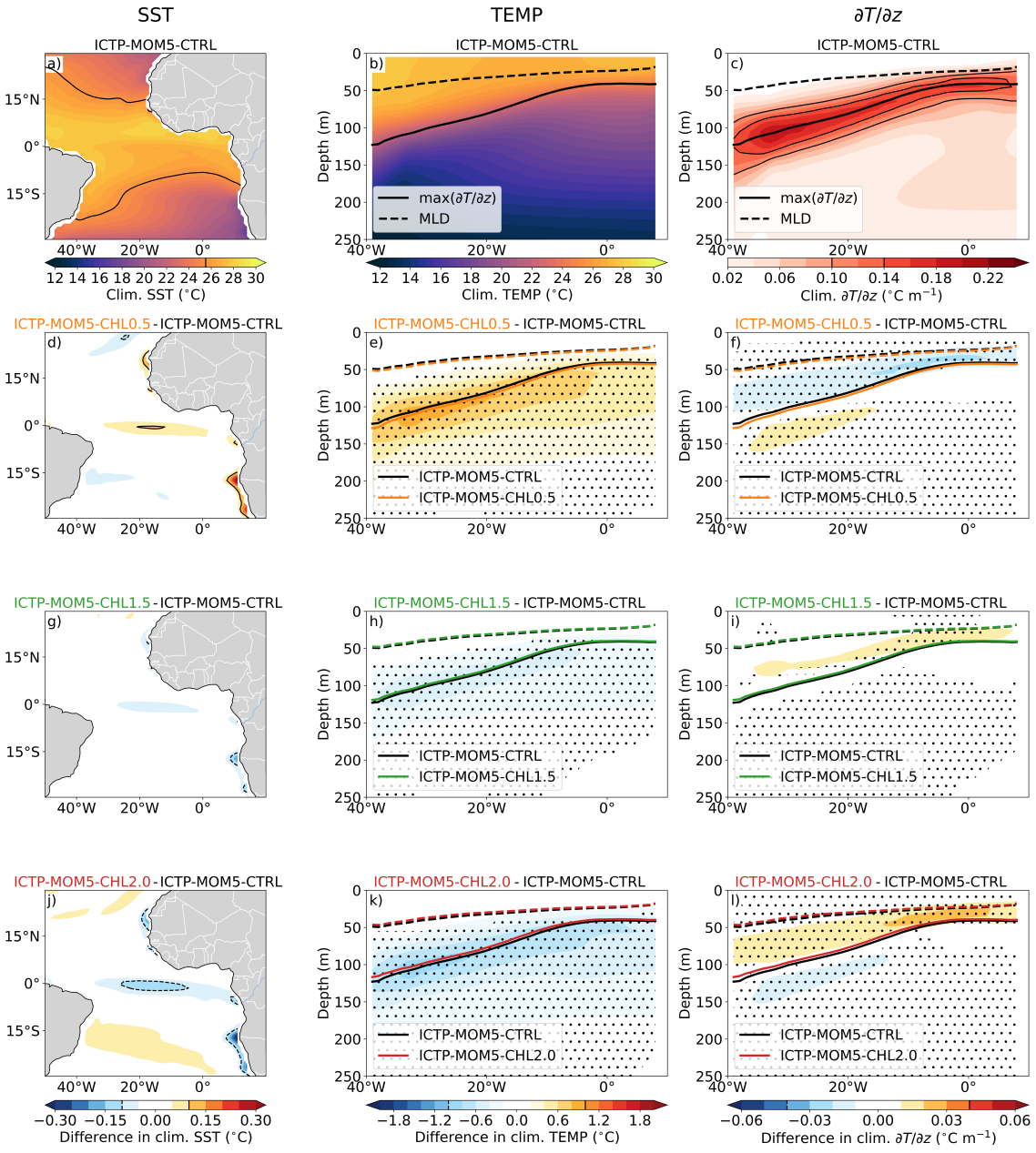


**Figure A1.** Climatological mean (a) SST, (b) temperature in the upper 250 m of the equatorial Atlantic (40°W-10°E; 3°S-3°N), and (c) vertical temperature gradient in the upper 250 of the equatorial Atlantic from ICTP-MOM5-CTRL over the period 1982-2020. In (b, c) the black thick dashed (continuous) line indicates the MLD (max($\partial T/\partial z$)). Difference between ICTP-MOM5-CHL0.5 and ICTP-MOM5-CTRL in terms of (d) SST, (e) temperature, and (f) vertical temperature gradient. (g, h, i) Same as (d, e, f) but between ICTP-MOM5-CHL1.5 and ICTP-MOM5-CTRL. (j, k, l) Same as (d, e, f) but between ICTP-MOM5-CHL2.0 and ICTP-MOM5-CTRL. Stipplings indicate regions where the difference in mean-state is significantly different according to a bootstrap test (see Sect. 2.2.3). We note that the range of the colorbars differ from Fig. 2.

https://doi.org/10.5194/egusphere-2026-2021
Preprint. Discussion started: 14 April 2026


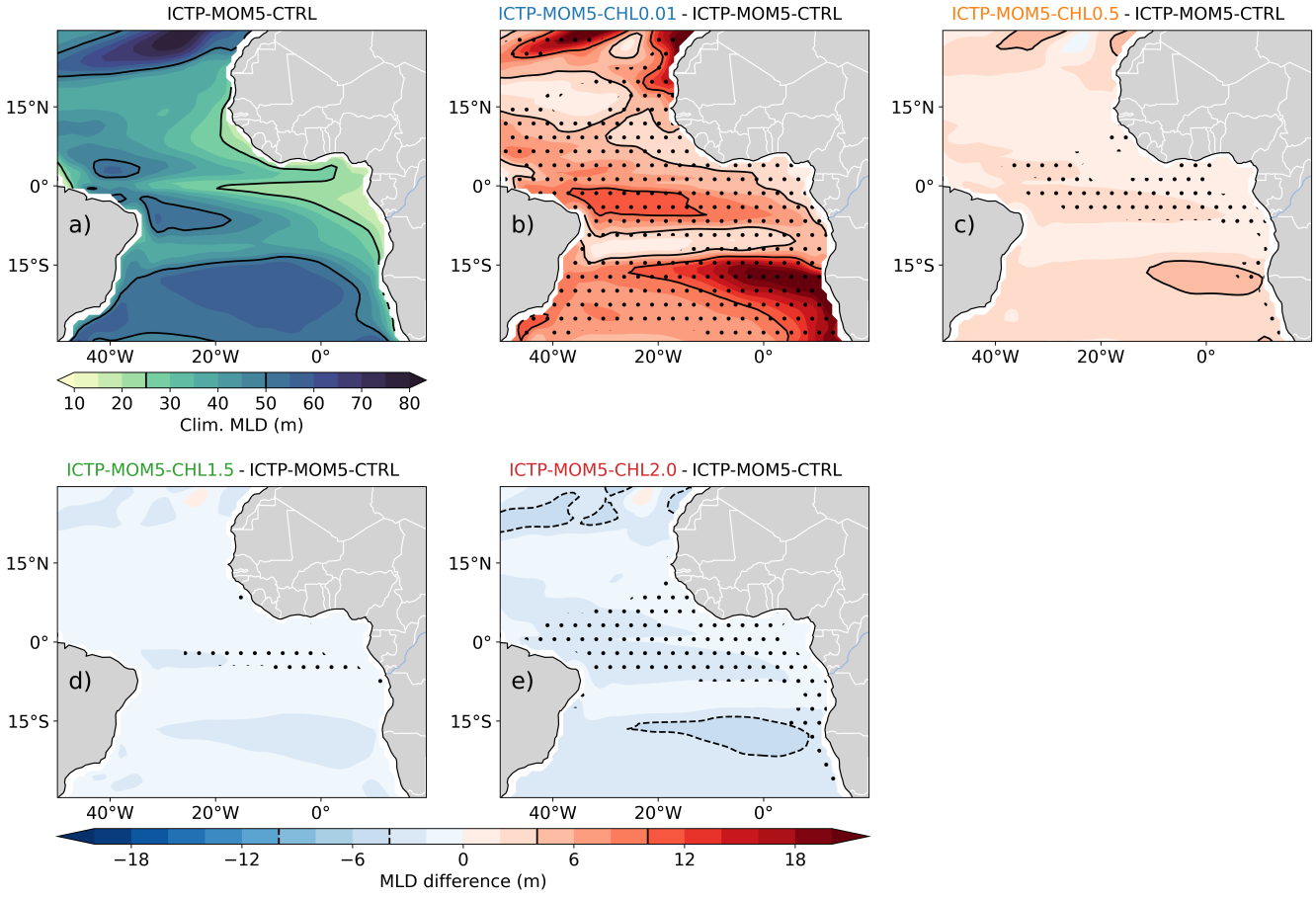


**Figure A2.** (a) Climatological mean tropical Atlantic mixed layer depth for ICTP-MOM5-CTRL. Black contours indicate the 25 m and 50 m MLDs. Difference in climatological mean MLD between between ICTP-MOM5-CTRL and (b) ICTP-MOM5-CHL0.01, (c) ICTP-MOM5-CHL0.5, (d) ICTP-MOM5-CHL1.5, and (e) ICTP-MOM5-CHL2.0. Dashed (solid) black contours indicate the -10 m and -4 m (4 m and 10 m) differences.

https://doi.org/10.5194/egusphere-2026-2021
Preprint. Discussion started: 14 April 2026


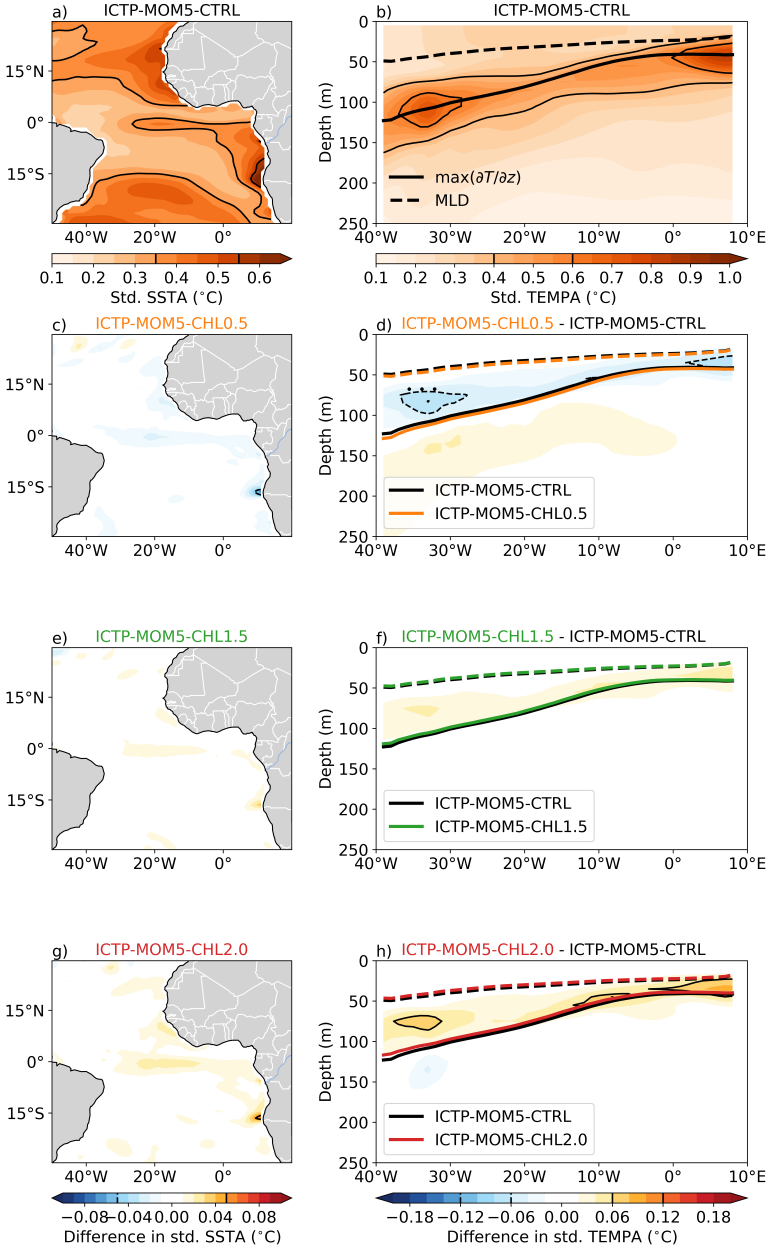


**Figure A3.** Standard deviation of (a) detrended SSTA, (b) temperature anomalies in the upper 250 m of the equatorial Atlantic (40°W-10°E; 3°S-3°N) from ICTP-MOM5-CTRL over the period 1982-2020. In (b) the black thick dashed (continuous) line indicates the MLD (max($\partial T/\partial z$)). Difference between ICTP-MOM5-CHL0.5 and ICTP-MOM5-CTRL in terms of (d) SST and (e) temperature variability. In (c) black dashed (solid) contours indicate -0.05 °C (0.05 °C). In (d) black dashed (solid) contours indicate -0.12 °C and -0.06 °C (0.06 °C and 0.12 °C). (e, f) Same as (c, d) but between ICTP-MOM5-CHL1.5 and ICTP-MOM5-CTRL. (g, h) Same as (c, d) but between ICTP-MOM5-CHL2.0 and ICTP-MOM5-CTRL. Stipplings indicate regions where the difference in mean-state is significantly different according to a bootstrap test (see Sect. 2.2.3). We note that the range of the colorbars differ from Fig. 4.

https://doi.org/10.5194/egusphere-2026-2021
Preprint. Discussion started: 14 April 2026


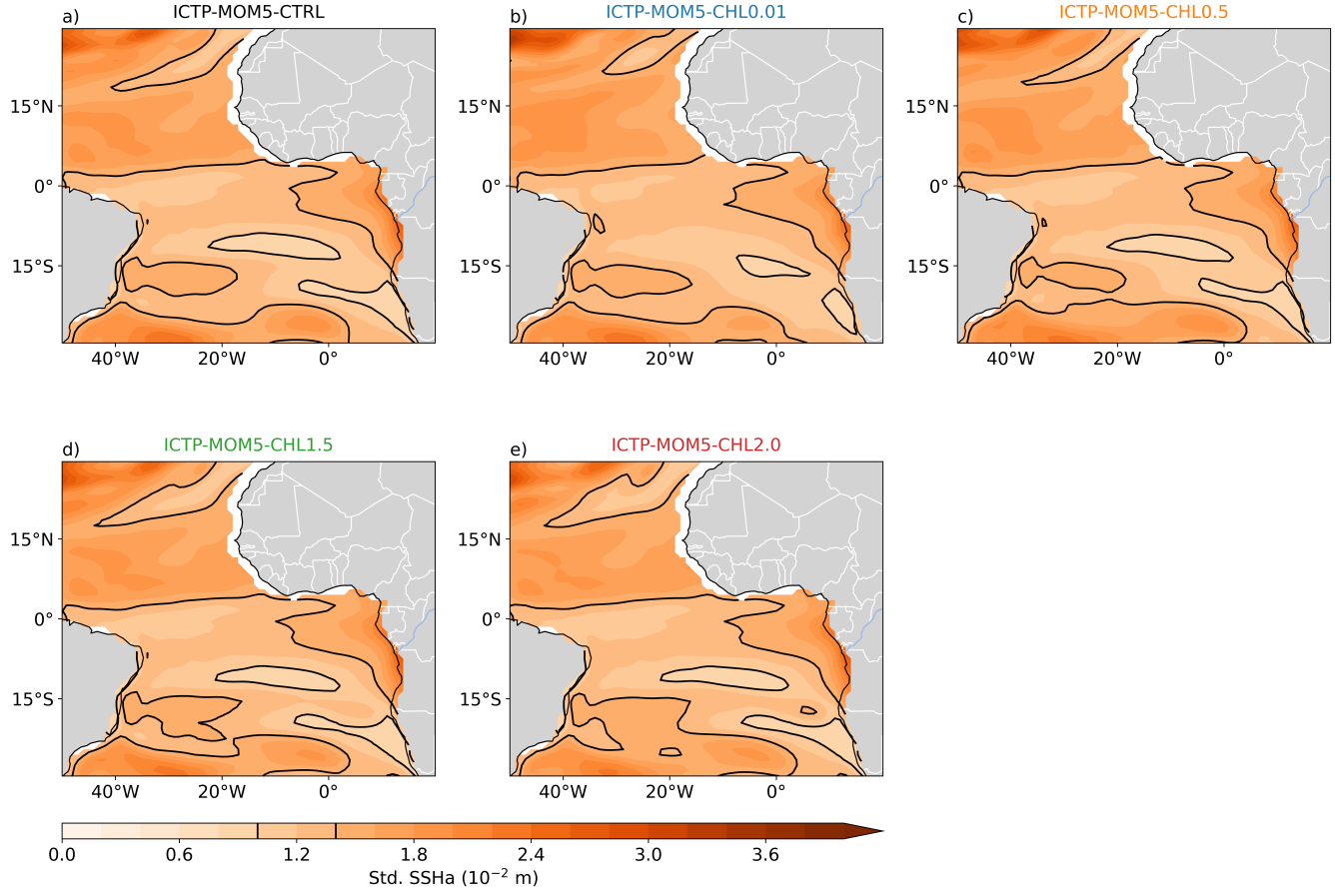


**Figure A4.** Standard deviation of detrended SSHA over the 1982-2020 for (a) ICTP-MOM5-CTRL, (b) ICTP-MOM5-CHL0.01, (c) ICTP-MOM5-CHL0.5, (d) ICTP-MOM5-CHL1.5, and (e) ICTP-MOM5-CHL2.0. Black contours denote the 0.01 m and 0.014 m standard deviation levels.

https://doi.org/10.5194/egusphere-2026-2021
Preprint. Discussion started: 14 April 2026


## References

Anderson, W. G., Gnanadesikan, A., Hallberg, R., Dunne, J., and Samuels, B. L.: Impact of ocean color on the maintenance of the Pacific Cold Tongue, Geophysical Research Letters, 34, https://doi.org/https://doi.org/10.1029/2007GL030100, 2007.

Anderson, W. G., Gnanadesikan, A., and Wittenberg, A.: Regional impacts of ocean color on tropical Pacific variability, Ocean Sci., 5, 313–327, https://doi.org/10.5194/os-5-313-2009, 2009.

Bjerknes, J.: ATMOSPHERIC TELECONNECTIONS FROM THE EQUATORIAL PACIFIC, Monthly Weather Review, 97, 163 – 172, https://doi.org/https://doi.org/10.1175/1520-0493(1969)097<0163:ATFTEP>2.3.CO;2, 1969.

Brandt, P., Caniaux, G., Bourlès, B., Lazar, A., Dengler, M., Funk, A., Hormann, V., Giordani, H., and Marin, F.: Equatorial upper-ocean dynamics and their interaction with the West African monsoon, Atmospheric Science Letters, 12, 24–30, https://doi.org/https://doi.org/10.1002/asl.287, 2011.

Brandt, P., Alory, G., Awo, F. M., Dengler, M., Djakouré, S., Imbol Koungue, R. A., Jouanno, J., Körner, M., Roch, M., and Rouault, M.: Physical processes and biological productivity in the upwelling regions of the tropical Atlantic, Ocean Science, 19, 581–601, https://doi.org/10.5194/os-19-581-2023, 2023.

Brandt, P., Körner, M., Moum, J. N., Roch, M., Subramaniam, A., Czeschel, R., Krahmann, G., Dengler, M., and Kiko, R.: Seasonal productivity of the equatorial Atlantic shaped by distinct wind-driven processes, Nature Geoscience, 18, 84–90, 2025.

Caniaux, G., Giordani, H., Redelsperger, J.-L., Guichard, F., Key, E., and Wade, M.: Coupling between the Atlantic cold tongue and the West African monsoon in boreal spring and summer, Journal of Geophysical Research: Oceans, 116, https://doi.org/https://doi.org/10.1029/2010JC006570, 2011.

Chenillat, F., Illig, S., Jouanno, J., Awo, F. M., Alory, G., and Brehmer, P.: How do Climate Modes Shape the Chlorophyll-a Interannual Variability in the Tropical Atlantic?, Geophysical Research Letters, 48, e2021GL093 769, https://doi.org/https://doi.org/10.1029/2021GL093769, e2021GL093769 2021GL093769, 2021.

Copernicus: Global Ocean Colour (Copernicus-GlobColour), Bio-Geo-Chemical, L4 (monthly and interpolated) from Satellite Observations (1997–ongoing), https://doi.org/10.48670/moi-00281, accessed on 22-01-2026, 2024.

Farneti, R.: ICTP-MOM5 driven by JRA55-do surface dataset with different Chl-a values, https://doi.org/10.5281/zenodo.11047949, 2026.

Farneti, R., Stiz, A., and Ssebandeke, J. B.: Improvements and persistent biases in the southeast tropical Atlantic in CMIP models, npj Climate and Atmospheric Science, 5, 42, https://doi.org/10.1038/s41612-022-00264-4, 2022.

Fox-Kemper, B., Ferrari, R., and Hallberg, R.: Parameterization of Mixed Layer Eddies. Part I: Theory and Diagnosis, Journal of Physical Oceanography, 38, 1145 – 1165, https://doi.org/https://doi.org/10.1175/2007JPO3792.1, 2008.

Fox-Kemper, B., Danabasoglu, G., Ferrari, R., Griffies, S., Hallberg, R., Holland, M., Maltrud, M., Peacock, S., and Samuels, B.: Parameterization of mixed layer eddies. III: Implementation and impact in global ocean climate simulations, Ocean Modelling, 39, 61–78, https://doi.org/https://doi.org/10.1016/j.ocemod.2010.09.002, modelling and Understanding the Ocean Mesoscale and Submesoscale, 2011.

Frouin, R., Ueyoshi, K., and Kampel, M.: Influence of solar radiation absorbed by phytoplankton on the thermal structure and circulation of the tropical Atlantic Ocean, in: Coastal Ocean Remote Sensing, edited by Frouin, R. J. and Lee, Z., vol. 6680, p. 668015, International Society for Optics and Photonics, SPIE, https://doi.org/10.1117/12.738969, 2007.

Gent, P. R. and Mcwilliams, J. C.: Isopycnal Mixing in Ocean Circulation Models, Journal of Physical Oceanography, 20, 150 – 155, https://doi.org/https://doi.org/10.1175/1520-0485(1990)020<0150:IMIOCM>2.0.CO;2, 1990.

https://doi.org/10.5194/egusphere-2026-2021
Preprint. Discussion started: 14 April 2026


Gent, P. R., Willebrand, J., McDougall, T. J., and McWilliams, J. C.: Parameterizing Eddy-Induced Tracer Transports in Ocean Circulation Models, Journal of Physical Oceanography, 25, 463 – 474, https://doi.org/https://doi.org/10.1175/1520-0485(1995)025<0463:PEITTI>2.0.CO;2, 1995.

Gnanadesikan, A. and Anderson, W. G.: Ocean Water Clarity and the Ocean General Circulation in a Coupled Climate Model, Journal of Physical Oceanography, 39, 314–332, https://doi.org/https://doi.org/10.1175/2008JPO3935.1, 2009.

Griffies, S. M.: The Gent–McWilliams Skew Flux, Journal of Physical Oceanography, 28, 831 – 841, https://doi.org/https://doi.org/10.1175/1520-0485(1998)028<0831:TGMSF>2.0.CO;2, 1998.

Griffies, S. M.: Elements of the Modular Ocean Model (MOM) (2012 Release), GFDL Ocean Group Technical Report No.7, NOAA/Geophysical Fluid Dynamics Laboratory, 618 + xiii pages, 2012.

Grodsky, S. A., Carton, J. A., and McClain, C. R.: Variability of upwelling and chlorophyll in the equatorial Atlantic, Geophysical Research Letters, 35, https://doi.org/https://doi.org/10.1029/2007GL032466, 2008.

Hernandez, O., Jouanno, J., Echevin, V., and Aumont, O.: Modification of sea surface temperature by chlorophyll concentration in the Atlantic upwelling systems, Journal of Geophysical Research: Oceans, 122, 5367–5389, https://doi.org/https://doi.org/10.1002/2016JC012330, 2017.

Hirst, A. C. and Hastenrath, S.: Atmosphere-Ocean Mechanisms of Climate Anomalies in the Angola-Tropical Atlantic Sector, Journal of Physical Oceanography, 13, 1146 – 1157, https://doi.org/https://doi.org/10.1175/1520-0485(1983)013<1146:AOMOCA>2.0.CO;2, 1983.

Hong, Z., Long, D., Shan, K., Zhang, J.-M., Woolway, R. I., Liu, M., Mann, M. E., and Fang, H.: Declining ocean greenness and phytoplankton blooms in low to mid-latitudes under a warming climate, Science Advances, 11, eadx4857, https://doi.org/10.1126/sciadv.adx4857, 2025.

Imbol Koungue, R. A., Brandt, P., Prigent, A., Aroucha, L. C., Lübbecke, J., Imbol Nkwinkwa, A. S. N., Dengler, M., and Keenlyside, N.: Drivers and impact of the 2021 extreme warm event in the tropical Angolan upwelling system, Scientific Reports, 14, 16 824, https://doi.org/10.1038/s41598-024-67569-7, 2024.

Imbol Koungue, R. A., Prigent, A., Lübbecke, J. F., Brandt, P., and Jouanno, J.: Interannual variability of net primary productivity in the northwest African coastal upwelling system and their relation to Dakar Niños, Scientific Reports, 15, 43 875, https://doi.org/10.1038/s41598-025-31860-y, 2025.

Jochum, M., Yeager, S., Lindsay, K., Moore, K., and Murtugudde, R.: Quantification of the Feedback between Phytoplankton and ENSO in the Community Climate System Model, Journal of Climate, 23, 2916–2925, https://doi.org/https://doi.org/10.1175/2010JCLI3254.1, 2010.

Keenlyside, N. S. and Latif, M.: Understanding Equatorial Atlantic Interannual Variability, Journal of Climate, 20, 131 – 142, https://doi.org/https://doi.org/10.1175/JCLI3992.1, 2007.

Koseki, S., Tjiputra, J., Fransner, F., Crespo, L. R., and Keenlyside, N. S.: Disentangling the impact of Atlantic Niño on sea-air CO2 flux, Nature Communications, 14, 3649, https://doi.org/10.1038/s41467-023-38718-9, 2023.

Kucharski, F., Bracco, A., Yoo, J. H., and Molteni, F.: Atlantic forced component of the Indian monsoon interannual variability, Geophysical Research Letters, 35, https://doi.org/https://doi.org/10.1029/2007GL033037, 2008.

Large, W. G., McWilliams, J. C., and Doney, S. C.: Oceanic vertical mixing: A review and a model with a nonlocal boundary layer parameterization, Reviews of Geophysics, 32, 363–403, https://doi.org/https://doi.org/10.1029/94RG01872, 1994.

Lengaigne, M., Menkes, C., Aumont, O., Gorgues, T., Bopp, L., André, J.-M., and Madec, G.: Influence of the oceanic biology on the tropical Pacific climate in a coupled general circulation model, Climate Dynamics, 28, 503–516, https://doi.org/10.1007/s00382-006-0200-2, 2007.

https://doi.org/10.5194/egusphere-2026-2021
Preprint. Discussion started: 14 April 2026


Lewis, M. R., Carr, M.-E., Feldman, G. C., Esaias, W., and McClain, C.: Influence of penetrating solar radiation on the heat budget of the equatorial Pacific Ocean, Nature, 347, 543–545, https://doi.org/10.1038/347543a0, 1990.

Löptien, U., Eden, C., Timmermann, A., and Dietze, H.: Effects of biologically induced differential heating in an eddy-permitting coupled ocean-ecosystem model, Journal of Geophysical Research: Oceans, 114, https://doi.org/https://doi.org/10.1029/2008JC004936, 2009.

Lübbecke, J. F., Rodríguez-Fonseca, B., Richter, I., Martín-Rey, M., Losada, T., Polo, I., and Keenlyside, N. S.: Equatorial Atlantic variability—Modes, mechanisms, and global teleconnections, WIREs Climate Change, 9, e527, https://doi.org/https://doi.org/10.1002/wcc.527, 2018.

Manizza, M., Le Quéré, C., Watson, A. J., and Buitenhuis, E. T.: Bio-optical feedbacks among phytoplankton, upper ocean physics and sea-ice in a global model, Geophysical Research Letters, 32, https://doi.org/https://doi.org/10.1029/2004GL020778, 2005.

Marzeion, B., Timmermann, A., Murtugudde, R., and Jin, F.-F.: Biophysical Feedbacks in the Tropical Pacific, Journal of Climate, 18, 58–70, https://doi.org/https://doi.org/10.1175/JCLI3261.1, 2005.

Morel, A.: Optical modeling of the upper ocean in relation to its biogenous matter content (case I waters), Journal of Geophysical Research: Oceans, 93, 10 749–10 768, https://doi.org/https://doi.org/10.1029/JC093iC09p10749, 1988.

Morel, A. and Antoine, D.: Heating Rate within the Upper Ocean in Relation to its Bio–optical State, Journal of Physical Oceanography, 24, 1652–1665, https://doi.org/https://doi.org/10.1175/1520-0485(1994)024<1652:HRWTUO>2.0.CO;2, 1994.

Murtugudde, R., Beauchamp, J., McClain, C. R., Lewis, M., and Busalacchi, A. J.: Effects of Penetrative Radiation on the Upper Tropical Ocean Circulation, Journal of Climate, 15, 470–486, https://doi.org/https://doi.org/10.1175/1520-0442(2002)015<0470:EOPROT>2.0.CO;2, 2002.

Nakamoto, S., Kumar, S. P., Oberhuber, J. M., Ishizaka, J., Muneyama, K., and Frouin, R.: Response of the equatorial Pacific to chlorophyll pigment in a mixed layer isopycnal ocean general circulation model, Geophysical Research Letters, 28, 2021–2024, https://doi.org/https://doi.org/10.1029/2000GL012494, 2001.

Oettli, P., Morioka, Y., and Yamagata, T.: A Regional Climate Mode Discovered in the North Atlantic: Dakar Niño/Niña, Scientific Reports, 6, 18 782, https://doi.org/10.1038/srep18782, 2016.

Okumura, Y. and Xie, S.-P.: Some Overlooked Features of Tropical Atlantic Climate Leading to a New Niño-Like Phenomenon, Journal of Climate, 19, 5859 – 5874, https://doi.org/10.1175/JCLI3928.1, 2006.

Park, J.-Y., Kug, J.-S., and Park, Y.-G.: An exploratory modeling study on bio-physical processes associated with ENSO, Progress in Oceanography, 124, 28–41, https://doi.org/https://doi.org/10.1016/j.pocean.2014.03.013, 2014a.

Park, J.-Y., Kug, J.-S., Seo, H., and Bader, J.: Impact of bio-physical feedbacks on the tropical climate in coupled and uncoupled GCMs, Climate Dynamics, 43, 1811–1827, https://doi.org/10.1007/s00382-013-2009-0, 2014b.

Paulson, C. A. and Simpson, J. J.: Irradiance Measurements in the Upper Ocean, Journal of Physical Oceanography, 7, 952–956, https://doi.org/https://doi.org/10.1175/1520-0485(1977)007<0952:IMITUO>2.0.CO;2, 1977.

Prigent, A. and Farneti, R.: An assessment of equatorial Atlantic interannual variability in Ocean Model Intercomparison Project (OMIP) simulations, Ocean Science, 20, 1067–1086, https://doi.org/10.5194/os-20-1067-2024, 2024.

Prigent, A., Lübbecke, J. F., Bayr, T., Latif, M., and Wengel, C.: Weakened SST variability in the tropical Atlantic Ocean since 2000, Climate Dynamics, 54, 2731–2744, https://doi.org/10.1007/s00382-020-05138-0, 2020.

Reynolds, R. W., Smith, T. M., Liu, C., Chelton, D. B., Casey, K. S., and Schlax, M. G.: Daily High-Resolution-Blended Analyses for Sea Surface Temperature, Journal of Climate, 20, 5473 – 5496, https://doi.org/10.1175/2007JCLI1824.1, 2007.

https://doi.org/10.5194/egusphere-2026-2021
Preprint. Discussion started: 14 April 2026


Richter, I. and Tokinaga, H.: 7 - The Atlantic zonal mode: Dynamics, thermodynamics, and teleconnections, in: Tropical and Extratropical Air-Sea Interactions, edited by Behera, S. K., pp. 171–206, Elsevier, ISBN 978-0-12-818156-0, https://doi.org/https://doi.org/10.1016/B978-0-12-818156-0.00008-3, 2021.

Richter, I., Xie, S.-P., Wittenberg, A. T., and Masumoto, Y.: Tropical Atlantic biases and their relation to surface wind stress and terrestrial precipitation, Climate Dynamics, 38, 985–1001, https://doi.org/10.1007/s00382-011-1038-9, 2012.

Servain, J., Picaut, J., and Merle, J.: Evidence of Remote Forcing in the Equatorial Atlantic Ocean, Journal of Physical Oceanography, 12, 457 – 463, https://doi.org/https://doi.org/10.1175/1520-0485(1982)012<0457:EORFIT>2.0.CO;2, 1982.

Shannon, L. V., Boyd, A. J., Brundrit, G. B., and Taunton-Clark, J.: On the existence of an El Niño-type phenomenon in the Benguela System, Journal of Marine Research, 44, 495–520, https://doi.org/doi:10.1357/002224086788403105, 1986.

Silsbe, G. M., Fox, J., Westberry, T. K., and Halsey, K. H.: Global declines in net primary production in the ocean color era, Nature Communications, 16, 5821, https://doi.org/10.1038/s41467-025-60906-y, 2025.

Strutton, P. G. and Chavez, F. P.: Biological Heating in the Equatorial Pacific: Observed Variability and Potential for Real-Time Calculation, Journal of Climate, 17, 1097–1109, https://doi.org/https://doi.org/10.1175/1520-0442(2004)017<1097:BHITEP>2.0.CO;2, 2004.

Sweeney, C., Gnanadesikan, A., Griffies, S. M., Harrison, M. J., Rosati, A. J., and Samuels, B. L.: Impacts of Shortwave Penetration Depth on Large-Scale Ocean Circulation and Heat Transport, Journal of Physical Oceanography, 35, 1103–1119, https://doi.org/https://doi.org/10.1175/JPO2740.1, 2005.

Timmermann, A. and Jin, F.-F.: Phytoplankton influences on tropical climate, Geophysical Research Letters, 29, 19–1–19–4, https://doi.org/https://doi.org/10.1029/2002GL015434, 2002.

Tsujino, H., Urakawa, S., Nakano, H., Small, R. J., Kim, W. M., Yeager, S. G., Danabasoglu, G., Suzuki, T., Bamber, J. L., Bentsen, M., Böning, C. W., Bozec, A., Chassignet, E. P., Curchitser, E., Boeira Dias, F., Durack, P. J., Griffies, S. M., Harada, Y., Ilicak, M., Josey, S. A., Kobayashi, C., Kobayashi, S., Komuro, Y., Large, W. G., Le Sommer, J., Marsland, S. J., Masina, S., Scheinert, M., Tomita, H., Valdivieso, M., and Yamazaki, D.: JRA-55 based surface dataset for driving ocean–sea-ice models (JRA55-do), Ocean Modelling, 130, 79–139, https://doi.org/https://doi.org/10.1016/j.ocemod.2018.07.002, 2018.

Wetzel, P., Maier-Reimer, E., Botzet, M., Jungclaus, J., Keenlyside, N., and Latif, M.: Effects of Ocean Biology on the Penetrative Radiation in a Coupled Climate Model, Journal of Climate, 19, 3973–3987, https://doi.org/https://doi.org/10.1175/JCLI3828.1, 2006.

Yoder, J. A. and Kennelly, M. A.: Seasonal and ENSO variability in global ocean phytoplankton chlorophyll derived from 4 years of SeaWiFS measurements, Global Biogeochemical Cycles, 17, https://doi.org/https://doi.org/10.1029/2002GB001942, 2003.

Zebiak, S. E.: Air–Sea Interaction in the Equatorial Atlantic Region, Journal of Climate, 6, 1567 – 1586, https://doi.org/https://doi.org/10.1175/1520-0442(1993)006<1567:AIITEA>2.0.CO;2, 1993.

Zhao, H., Manizza, M., Lozier, M. S., and Cassar, N.: Greener green and bluer blue: Ocean poleward greening over the past two decades, Science, 388, 1337–1340, https://doi.org/10.1126/science.adr9715, 2025.